International Specialty Conference on Cold-Formed Steel Structures

Wei-Wen Yu International Specialty Conference on Cold-Formed Steel Structures 2018

Nov 7th, 12:00 AM - Nov 8th, 12:00 AM

Seismic Behavior of Cold-Formed Steel Shear Walls during Full-Scale Building Shake Table Tests

X. Wang

Tara C. Hutchinson

G. Hegemier

Colin A. Rogers

Wei-Wen Yu International Specialty Conference on Cold-Formed Steel Structures
St. Louis, Missouri, U.S.A., November 7 & 8, 2018

Seismic behavior of cold-formed steel shear walls during full-scale building shake table tests

Wang, X.[1], Hutchinson, T.C.[2], and Hegemier, G.[3]

Abstract

Cold-formed steel sheathed shear walls are now emerging as a strategic vertical lateral load resisting component in seismic design. However, although a number of component cyclic test programs have been conducted in recent years to characterize their hysteretic behavior and guide design, system-level test programs to investigate their performance are so far lacking in the literature. To this end, a unique full-scale CFS-framed mid-rise building shake table test program was conducted to contribute to understanding the behavior of mid-rise cold-formed steel (CFS) wall-braced buildings under a multi-hazard scenario. The centerpiece of this project involved earthquake and live fire testing of a full-scale six-story CFS wall braced building constructed on the Large High Performance Outdoor Shake Table (LHPOST) at UCSD. This paper first provides a brief overview of the test program and summarizes the system-level (global) response of the test building during the shake table tests. Subsequently, a key focus of this paper is comparison of the component-level responses of various shear wall systems of the test building as well as their physical damage.

1 Introduction

Growth in the use of cold-formed steel (CFS) framed construction has been substantial in recent years, perhaps most notably in high seismic regions in the western United States. Structural systems of this kind consist of repetitively framed light-gauge steel members (e.g., studs, tracks, joists) attached with sheathing materials (e.g., wood, sheet steel) to form wall-braced component.

[1] Post-doctoral Researcher, Univ. of California, San Diego, La Jolla, CA 92093-0085 (xiw002@ucsd.edu)
[2] Professor, Univ. of California, San Diego, La Jolla, CA 92093-0085 (tara@ucsd.edu)
[3] Distinguished Professor, Univ. of California, San Diego, La Jolla, CA 92093-0085 (ghegemier@ucsd.edu)

CFS-framed structures can offer lower installation and maintenance costs than other structural types, particularly when erected with prefabricated assemblies. They are also durable, formed of an inherently ductile material of consistent behavior, lightweight, and manufactured from recycled materials. Compared to other lightweight framing solutions, CFS is non-combustible, an important basic characteristic to minimize fire spread. While these lightweight systems provide the potential to support the need for resilient and sustainable housing, the state of understanding regarding their structural behavior in response to extreme events, in particular earthquakes and ensuing hazards, remains relatively limited.

In the past few decades, a number of experimental investigations have been devoted to advancing understanding regarding the seismic response of CFS-framed shear walls. The work conducted by Serrette et al. (1997) represents one of the first efforts of its kind in North America to study the seismic response of CFS-framed shear walls. This effort largely formed the initial basis for codified design of CFS systems (e.g., AISI, 2007 and 2012). Research of this kind was later extended to investigate CFS wall behavior with varied sheathing materials or framing details. These experimental studies included pseudo-static tests of CFS-framed steel strap shear walls (Al-Kharat and Rogers, 2007) and steel-sheet shear walls (Balh et al., 2014), as well as pseudo-dynamic tests of two-story steel-sheet shear wall assemblies (Shamin et al., 2013). In addition, recent studies involved testing of CFS shear walls sheathed with sheet steel (Yu, 2010) or oriented strand board panels (Liu et al., 2014). In contrast, there is a paucity of data regarding the seismic response of CFS-framed buildings configured in their system-level arrangement (whole building tests). Assessing the behavior of this critical structural component in its multi-story setting as configured within a building is important as the interstory drift and floor accelerations will vary during an earthquake.

To this end, a unique multidisciplinary test project was conducted on the LHPOST test facility at UCSD in 2016 (Wang et al., 2016 and 2018; Hutchinson et al., 2017). Central to this research is the system-level earthquake and fire testing of a full-scale six-story CFS wall braced building. Within a three-week test program, the CFS test building was subjected to seven earthquake tests of increasing motion intensity before and two earthquake tests after the live fire tests conducted at two select levels (level 2 and 6) of the building. This paper briefly summarizes the overall test program as well as the system-level (global) response of the test building during the test program. Subsequently, a focus herein is comparison of the component-level responses of various shear wall systems of the test building. As a result of the length limitation, discussions of the shear wall behavior characteristics are restricted to those during pre-fire earthquake test phase. Additional information on the test program as well as test results regarding the global building response and local shear wall behavior are available in Wang et al. (2018).

2 Building Design and Shear Wall Systems

2.1 Building Design

The CFS test building was assumed to be located in a high seismic region near downtown Los Angeles, with its design basis complying with current code provisions within ASCE 7-10 (ASCE, 2010), AISI S100 (AISI, 2012), and AISI S213 (AISI, 2007). As shown in Fig. 1, the building had a uniform plan dimension of 10.4 m × 7.3 m (34 ft × 24 ft) at occupying almost the entire 12.2 m × 7.6 m (40 ft × 25 ft) shake table footprint. The total height of the building was 19.2 m above the shake table platen, including a floor-to-floor height of 3.1 m (10 ft) for all stories and a 1.2 m-tall (4 ft tall) parapet on the roof perimeter. As a result, the code-based fundamental period of the test building T was determined as 0.43 sec considering a total building height of 18.3 m (60 ft) excluding the parapets. The base shear coefficient C_s of the building was consequently determined as 0.236 given a response modification factor R of 6.5. The estimated maximum inelastic story drift of the building was ~1.0% (with a deflection amplification factor C_d of 4.0), which was lower than the allowable story drift of 2.0% as prescribed in ASCE 7-10 (ASCE, 2010).

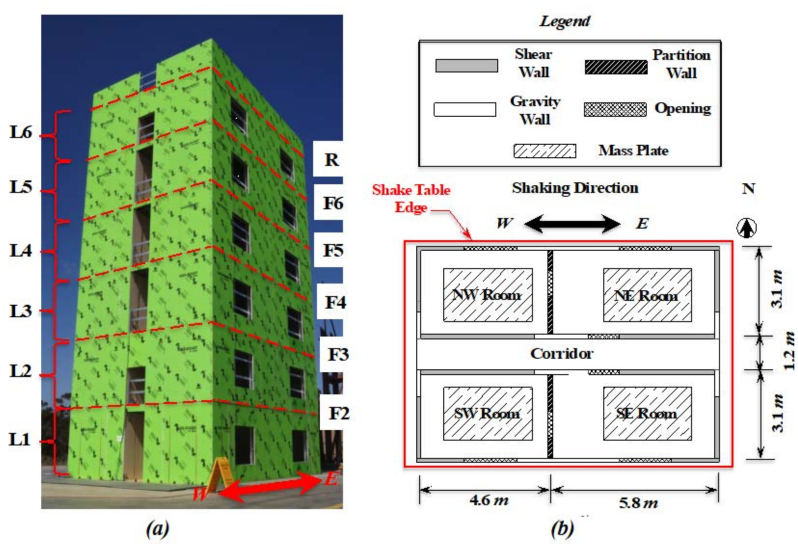

Figure 1. (a) Isometric view of test building, (b) building plan layout (typical of floor 2 to 6).

In terms of layout, the building had a symmetric floor plan with a 1.2 m (4 ft) wide corridor oriented along the longitudinal centerline and a room at each quadrant of the building (Fig. 1b). Two transverse partition walls were located ~0.6 m (2 ft) west of the transverse centerline (level 2 through 6), each separating the two rooms on the same side of the corridor. It is noted that no partition walls were installed at the first level to retain simplicity in attachment to the shake table. To account for the (seismic) live loads and the weight of certain architectural features excluded from construction (e.g., flooring, exterior façade finishing), four mass plates were installed on the floor diaphragm at each floor from the second floor through the roof. Each mass plate had a dimension of 3.0 m (10 ft) × 1.8 m (6 ft) and a weight of ~16.5 kN (3.7 kips).

2.2 Shear Wall Systems

The test building was detailed to carry lateral seismic loading using prefabricated repetitively framed CFS floors and walls with shear load resistance provided via steel sheathing. As shown in Fig. 1b, two longitudinal shear walls were placed along each (east and west) end of the corridor, with an associated wall length of 4.0 m (13 ft) for the walls at the west end and 3.3 m (11 ft). In addition, short shear walls with a length of ~1.6 m (5'-4") in the longitudinal direction and ~2.1 m (7 ft) in the transverse direction were placed at the four corners of the building. The total shear wall length per floor was 21.3 m (70 ft) in the longitudinal (shaking) direction and 8.6 m (28 ft) in the transverse direction. With the exception of the stick-framed structural walls at the first level, the structural walls and floor systems at all remaining levels (level 2 through 6) was constructed using prefabricated panels.

The shear walls were framed using standard framing members (e.g., studs, tracks). Sheathing materials utilized load-resisting structural panels on the exterior (or corridor) side and 16 mm (5/8") thick regular gypsum boards on the room side. The structural panels were fabricated using 16 mm (5/8") thick gypsum boards (or) bonded with a layer of 0.686 mm (0.027") thick (22 ga.) sheet steel to provide shear resistance to the shear wall assemblies. For the corridor shear walls (see Fig. 2a), vertical studs utilized 600S200-68 at 610 mm (24") o.c at the first level and 600S200-54 at 610 mm (24") o.c at all remaining levels. The (top and bottom) tracks were consistently constructed using 600T200-54, with the exception of the first level bottom tracks that used 600T200-97. The structural panels of the corridor walls were attached to framing using #8 self-tapping metal screws at 406 mm (16") o.c in field but different spacing on boundary: 76 mm (3") o.c. for the lower three levels, 102 mm (4") for level 4, and 152 mm (6") o.c for the upper two levels. Additionally, the gypsum boards were attached to the framing by #8 drywall screws at a spacing of 152 mm (6") o.c. on boundary and 406 mm (16") o.c in field. The details of the corner shear walls (see Fig. 2c) were similar to those of the corridor shear walls, except: (1) vertical studs utilized 600S200-54 at 610 mm (24") o.c at all levels, (2) structural panels utilized 16 mm (5/8") thick moisture-resistant gypsum boards instead of regular gypsum boards since they were located on the building exterior, and (3) screw spacing was 152 mm (6") o.c on the boundary and 406 mm (16") o.c in field at all levels.

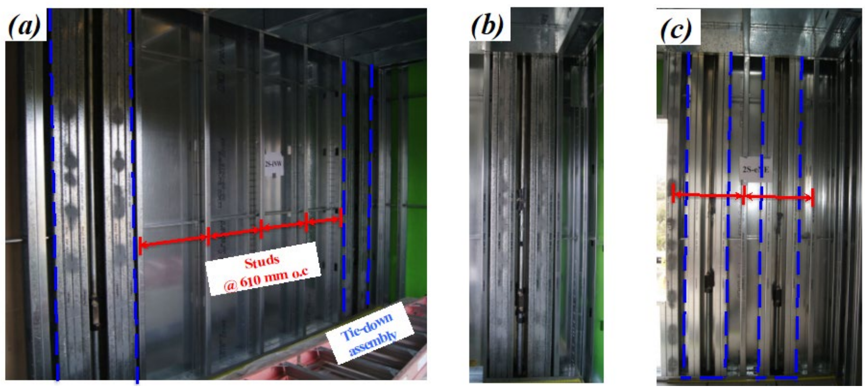

Figure 2. Shear walls framing at level 2: (a) corridor shear wall, (b) corridor shear wall tie-down subassembly, (c) longitudinal corner shear wall.

2.3 Shear Wall Tie-down Systems

Different from the uplift restraint systems adopted for typical low-rise CFS buildings, this mid-rise test building involved a tie-down system embedded within the corridor and corner shear walls, which spanned continuously over all levels of the building to resist the uplift forces. As shown in Fig. 2, each shear wall contained a pair of tie-down subassemblies at the two ends of the wall, which consisted of: (a) steel rods connected by couplers and spanned continuously over the entire height of the building, and (b) compression posts made of built-up stud packs. The tie-down rods were connected by couplers with double nut configuration located about 0.6 m (2 ft) above the floor level (Fig. 3b) and fastened to the floor using a bearing plate connection (Fig. 3c). It is noted that the distance between the tie-down rod pairs was ~0.6 m (2 ft) for the corner shear walls, resulting in an aspect ratio > 4:1 given a clear wall height of ~2.8 m (9'-2") excluding the diaphragm thickness. In contrast, the tie-down rod distance was ~3.0 m (10 ft) for the west corridor wall segments and ~2.4 m (8 ft) for the east corridor wall segments. Therefore, the aspect ratio of the corridor shear walls was about 1:1.

Two different types of steel rods were used as part of the tie-down system: (a) all-thread rods, and (b) smooth rods with threading only at the rod ends. These rods were fabricated using either ASTM A36 (plain finish) or ASTM A193 Grade B7 (zinc-coated) steel. Due to the different uplift force demands at individual shear walls, the tie-down rods and the compression posts varied significantly depending on their vertical and planar location. Complete details of the shear wall tie-down rods at three select levels are summarized in Table 1. In particular, the strength of the tie-down rods at these levels are compared with the measured tie-down rod axial forces as later discussed in Section 4.

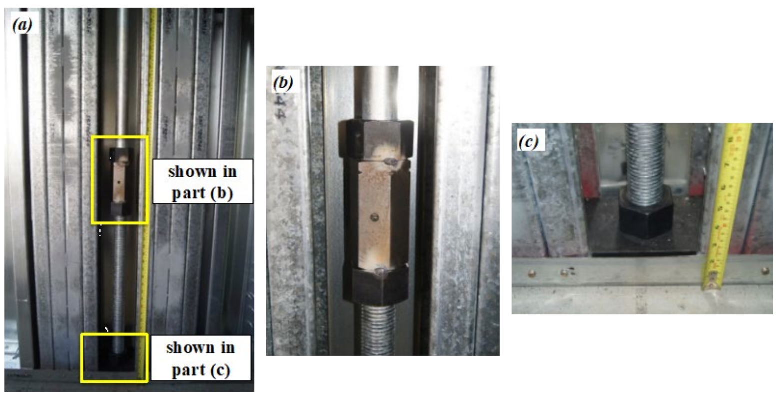

Figure 3. Tie-down rod connection details: (a) tie-down assembly (b) coupler and double nut connection, and (c) bearing plate connection.

Table 1. Specifications, cross section areas, and strength of the tie-down rods at level 1, 2, and 4.

Level #	Corridor shear wall			Corner shear wall		
	Designation	Diameter (mm)	F_u $[F_y]$ (kN)	Designation	Diameter (mm^2)	F_u $[F_y]$ (kN)
1	ASTM A722 (Grade 150)	46	1779 [1423]	ASTM A722 (Grade 150)	46	1779 [1423]
2	ASTM A193 (Grade B7)	43	1337 [1070]	ASTM A36	29	265 [170]
4	ASTM A193 (Grade B7)	29	553 [442]	ASTM A36	19	118 [71]

Notes: A_s – cross sectional area; F_u – ultimate tensile strength; F_y – yield tensile strength; Young's modulus of all steel products taken as 200 GPa.

2.4 Shear Wall Instrumentation

The test building consisted of a total of 17 instrumented shear walls at three select levels, namely, level 1, 2, and 4. As shown in Fig. 4a, the lower two levels each included three corridor shear walls (denoted as *SW-c*, *SE-c* and *NW-c*) and three corner (exterior) shear walls (denoted as *SW-e*, *SE-e* and *NE-e*), while level 4 consisted of five instrumented walls as the northeast corner shear wall was not instrumented due to difficulties related to wall exterior accessibility. As shown in Fig. 4b, instrumentation installed on these shear walls involved: (1) displacement transducers (i.e., string potentiometers and linear potentiometers) on the shear wall panels, and (2) strain gages on the tie-down steel rods. Interested readers are referred to Wang et al. (2018) for additional details of the shear wall instrumentation. Data recorded by these sensors provided local responses of individual shear walls in the following three categories:

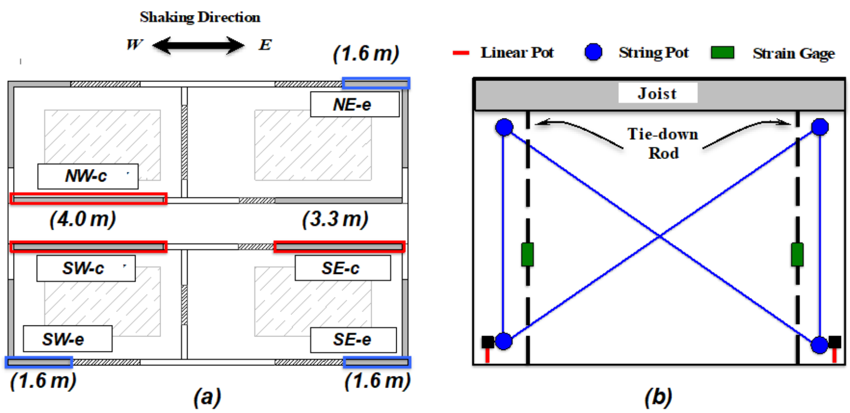

Figure 4. Shear wall instrumentation: (a) location of instrumented shear walls (typical of level 1, 2, and 4, length of individual wall specified in the parenthesis), (b) typical shear wall sensor configuration.

1. *Sheathing panel shear distortion:* measured using two diagonal and two vertically string potentiometers placed in a double-triangle configuration. Direct string potentiometer measurements were used to calculate the shear distortion (angle change of the triangles) of the shear wall structural panels. It is noted that the shape of the triangles varied as a result of the different shear wall dimensions.
2. *Tie-down rod axial forces:* measured using a pair of collocated strain gages (or a single strain gage) on the tie-down rods. Since the tie-down rods all remained elastic during the earthquake tests (as discussed later), the axial force of the tie-down rod is calculated by multiplying the measured strain of

the tie-down rod by its axial stiffness (product of sectional area and Young's modulus of steel).

3. *Wall end vertical displacements:* measured directly using two vertically oriented linear potentiometers at the base of the wall (one sensor at each wall end).

3 Test Protocol and Building Response

Within the three-week test program, the test building was subjected to seven earthquake tests of increasing motion intensity before and two earthquake tests after the live fire tests conducted at two select levels of the building. During the pre-fire earthquake test phase, the building was subjected to seven earthquake tests with increasing motion intensity levels, namely, serviceability (SLE), design (DE), and maximum considered earthquake (MCE) tests. Subsequently, a total of six live fire tests were conducted on the earthquake-damaged building at two select levels (four tests at level 2 and two at level 6) across a period of three consecutive days. The test program concluded with two post-fire earthquake tests (serviceability followed by MCE) on the final test day. It is noted that all the earthquake motions were applied in the east-west direction using the single-axis shake table, whose axis coincided with the geometric centroid of the longitudinal axis of the building.

Table 2 summarizes the peak building responses associated with individual earthquake tests, whereas the story shear versus interstory drift ratio (IDR) response during select earthquake tests are shown in Fig. 5. It is noted that the drift demands, such as peak interstory drift ratio (PIDRs) and peak roof drift ratios (PRDRs), serve as important proxies for assessing the performance of the building and individual shear walls. As shown in Fig. 5a, the story force displacement response of the building remained essentially linear during the serviceability level test (EQ2) while the story drift remained relatively small (PIDR < 0.1%). In contrast, the response became highly nonlinear as the drift demands reached ~1.0% during the design event (EQ6) and exceeded 1.5% during the MCE event (EQ7) (Fig. 5b-c). During the post-fire test phase, the final near-fault extreme event (EQ9) induced excessively large drift demands at level 2 of the building (PIDR > 12% and RDR_{res} > 1%), resulting in extremely severe damage to the structural walls at level 2. Despite the excessive damage, the building resisted collapse largely due to the presence of shear wall tie-down system (Hutchinson et al., 2017).

Table 2. Summary of test sequence and associated peak building responses

Test Date	Test Motion	EQ Target	*PFA* (g) (Floor #)	*PIDR* (%) (Level #)	*PRDR* (%)	RDR_{res} (%)
Day 1 (June 13, 2016)	EQ1:RIO-25	SLE	0.35 (R)	0.08 (L4)	0.05	0.0
	EQ2:CNP-25		0.38 (R)	0.09 (L4)	0.07	0.0
	EQ3:CUR-25		0.45 (R)	0.10 (L4)	0.08	0.0
Day 2 (June 13, 2016)	EQ4:CNP-25		0.43 (R)	0.10 (L4)	0.09	0.0
	EQ5:CNP-50	50% DE	0.85 (R)	0.24 (L3)	0.19	0.0
	EQ6:CNP-100	DE	2.07 (R)	0.89 (L4)	0.70	0.0
Day 3 (June 13, 2016)	EQ7:CNP-150	MCE	3.77 (F5)	1.70 (L4)	1.49	0.1
Fire Test Sequence (June 27–29, 2016)						
Day 4 (June 13, 2016)	EQ8:RIO-25	SLE	0.16 (R)	0.17 (L3)	0.12	0.0
	EQ9:RRS-150	MCE	4.43 (F5)	12.15 (L2)	2.84	1.2

Notes: *PFA*= peak floor acceleration; *PIDR* = peak interstory drift ratio; *PRDR* = peak roof drift ratio; RDR_{res} = residual roof drift ratio; SLE = serviceability earthquake; DE = design earthquake; MCE = maximum considered earthquake.

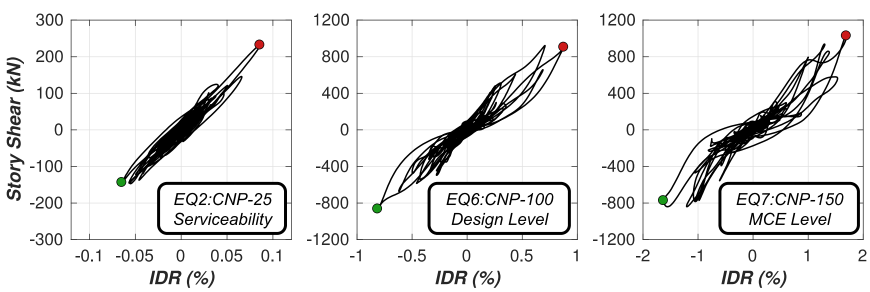

Figure 5. Story shear vs interstory drift ratio (IDR) response at level 4 during three select earthquake tests.

4 Seismic Response of Shear Wall Systems

Data measured from the shear walls at the three levels of the test building allowed for investigating the local shear wall responses during the earthquake tests as well as comparing the seismic behavior different shear walls dependent on the variations of specific wall details (corridor vs corner) or vertical locations. Herein, discussion focuses on only the shear wall response measured during the pre-fire earthquake test sequence. The measured time history responses of level 2 shear walls during the design event (EQ6) are first presented. Subsequently, the peak local responses of all the instrumented shear walls are summarized. It is noted that even though the seismic drift demand of the test building achieved its largest value at level 4 during the pre-fire earthquake tests (PIDR attained ~0.9% at level 4 compared with ~0.6% at level 2 during the design event EQ6), the measured local shear wall responses (e.g., tie-down rod forces, wall end displacements) were larger at level 2 than those of the level 4 shear walls.

Fig. 6 shows the measured local responses of the corridor shear wall pair (west and east segments on the south corridor wall line) at level 2 during the design event (EQ6). It is noted that the measured story drift at level 2 reached peak values of ~0.6% in both positive (eastward) and negative (westward) directions during this test (red circles represent the time instance when the story drift achieved the positive peak, whereas green circles correspond to that of the negative peak). With a peak story drift of ~0.6% at level 2, the peak shear distortion of the structural panels attained ~0.2% for the west wall segment and ~0.15% for east wall segment, accounting for 1/4 –1/3 of the peak story drift.

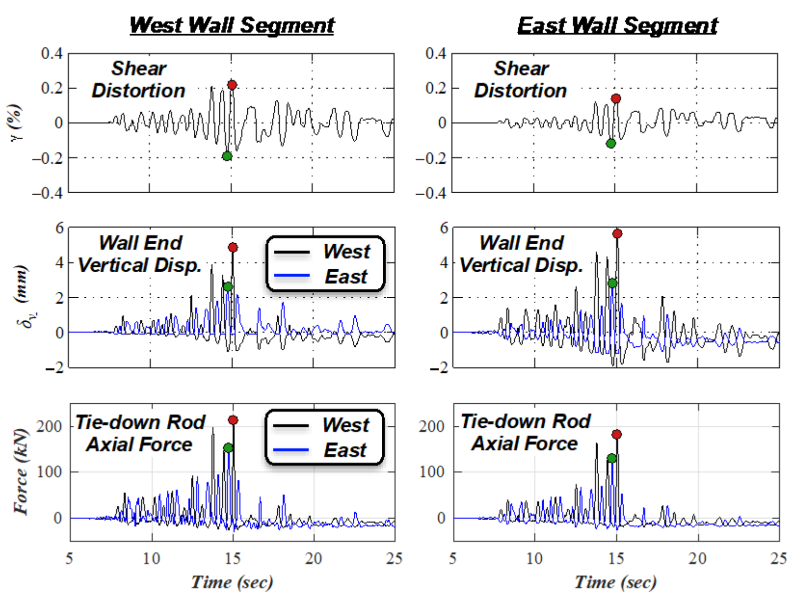

Figure 6. Local responses of the corridor shear wall pair at level 2 during the _design event (EQ6)_: panel shear distortions (first row), wall end vertical displacements (second row), and tie-down rod axial forces (third row).

As the story drift reached the positive (eastward) peak (denoted in red circles), the wall end vertical displacements and the tie-down rod tensile forces of both the east and west wall segments achieved their peak values at the west ends of the individual segments. In contrast, these local responses remained very small at the east ends of the two wall segments, since the east ends of both wall segments were characterized by compression in the vertical direction when the shear walls were subjected to peak story drift in the eastward direction. Similarly, when the story drift reached the negative (westward) peak (denoted in green circles), the peak wall end vertical displacements and peak tie-down rod tensile forces of both the east and west wall segments occurred at the east ends of shear walls. In addition, the shear walls at the two sides of the corridor (east and west segments) achieved comparable peak local responses associated with occurrence of the peak story drift. This indicates that the east and west corridor shear walls performed as individual wall segments (referred to as Type I system per AISI code provisions (AISI, 2007)) in response to seismic lateral loads. In addition, the tie-down rods of both wall segments achieved peak tensile forces of ~200 kN associated with the positive (eastward) peak story drift and < 150 kN associated with the negative (westward) peak story drift. The peak tensile forces of the tie-down rods were well below (~15%) their yield strength of 1337 kN (see Table 1) during the design event (EQ6).

Fig. 7 shows the measured responses of the longitudinal corner shear wall pair (southwest and southeast walls) at level 2 during the design event (EQ6). The shear force demands of the corner shear walls were much smaller than those of the corridor walls due to their much shorter length of the corner walls. As a result, the observed peak axial forces of the tie-down rods of the corner walls were substantially smaller than those of the corridor shear walls. The achieved peak wall end vertical displacements of the corner shear walls were only ~2 mm (compared to 5 mm for the corridor walls), whereas the peak tie-down rod axial forces were slightly larger than 60 kN (~40% their yield strength of 170 kN). In addition, the shear distortions of the corner shear walls were about 0.1%, which is smaller than those of the corridor shear walls (0.15% – 0.2 %). However, unlike the fact that the measured axial forces of the tie-down rods remained similar for the shear walls at the two ends of the corridor, the tie-down rod axial forces of the corner shear walls at the two sides of the building appeared less correlated. This is partially due to the interaction between the tie-down rods of the longitudinal corner shear walls with those of the adjacent transverse shear walls.

Fig. 8 presents the ratios of the peak shear distortions of shear wall structural panels over the PIDRs at the corresponding levels. It is noted that the positive (or negative) peak panel shear distortions are correlated with the corresponding

PIDR in the positive (or negative) directions. Comparison of the corridor walls with the corner walls indicates that the peak panel shear distortions of the corridor shear walls were consistently larger than those of the corner shear walls at the same level. For the shear walls at level 2, the panel shear distortions accounted for 20%~40% of the drift demands for the corridor walls but only about 20% for the corner walls. This may be attributed to the differences related to shear wall aspect ratios between the corridor and corner shear walls. The corner shear walls, which were much slenderer than the corridor shear walls, may lead to increased flexural deformation and reduced shear deformation contribution in response to lateral drift loading. In addition, the shear distortion ratios of the shear walls appeared to be smaller at higher levels. For instance, the shear distortions of the corridor wall structural panels accounted for 40~60% of the story drift at level 1, compared with 20~40% at level 4. This is likely attributed to the axial force demands of the tie-down rod systems, as the measured tensile forces of the tie-down rods of the level 4 shear walls was significantly smaller than those of the lower two levels.

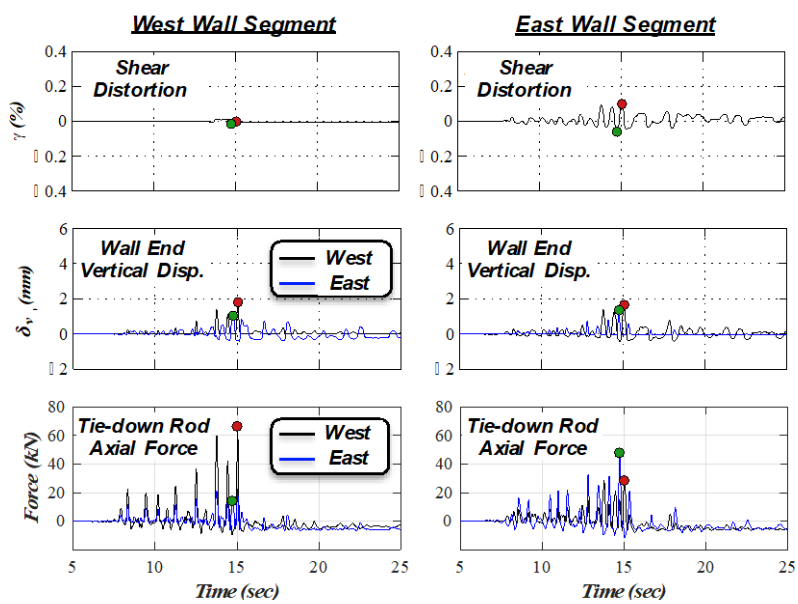

Figure 7. Local responses of the longitudinal corner shear wall pair at level 2 during the *design event (EQ6)*: panel shear distortions (first row), wall end vertical displacements (second row), and tie-down rod axial forces (third row).

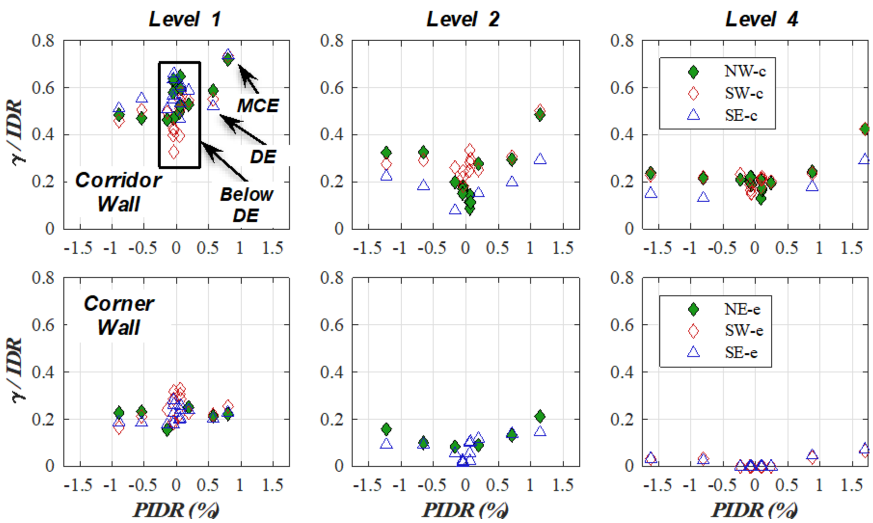

Figure 8. Normalized peak panel shear distortions of the corridor (first row) and corner (second row) shear walls during the pre-fire earthquake test sequence.

Fig. 9 summarizes the measured peak tensile forces of the corridor and corner shear wall tie-down rods during the pre-fire earthquake test phase. It is noted that the tie-down rod axial forces of the northwest corridor shear walls were not measured since no strain gages were installed on these walls. Data points associated with the positive (eastward) PIDRs represent those of the measured peak tensile forces of the tie-down rods at the west ends of individual shear walls, whereas those associated with the negative (westward) PIDRs represent the peak tensile forces of the tie-down rods at the east ends of the shear walls.

As a result of larger lateral force demands at the lower two levels, the measured peak tensile forces of the shear wall tie-down rods at the lower levels were much larger than those of the level 4 shear walls. The axial forces of the corridor walls at the lower two levels achieved ~400 kN but only 200 kN at level 4. In addition, the peak tensile forces of the corridor shear wall tie-down rods were much larger than those of the corner shear walls at the same level. The achieved peak tensile forces remained comparable for the corridor shear wall pairs (east and west wall segments) each of the three levels, while the forces differed apparently for the corner shear wall pairs. It is also important to note that the measured axial forces of all instrumented tie-down rods remained smaller than their respective yield strengths. During the pre-fire test phase, the tensile forces of the corridor shear wall tie-down rods reached only ~40% their respective yield strength, while those of the corner shear walls attained about 60%.

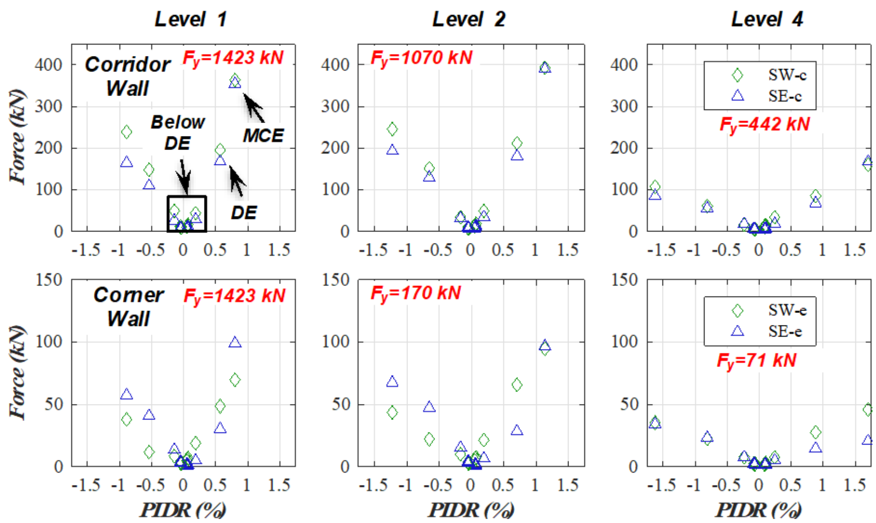

Figure 9. Peak tie-down rod tensile forces the corridor (first row) and corner (second row) shear walls during the pre-fire earthquake test sequence.

5 Physical Observations of Damage to Shear Walls

The shear walls systems at all levels performed satisfactorily during the pre-fire earthquake tests. Following the completion of the pre-fire earthquake tests with the PIDR exceeding 1% at all except the uppermost levels, representative damage observed at the corridor shear walls involved extensive screw withdrawal, sheathing crushing due to interactions with the adjacent gravity walls, as well as local buckling steel sheathing of the structural panels (with limited). As a result of smaller shear panel distortion demands for the corner (exterior) shear walls (see Fig. 8), damage associated with the corner shear walls was much less severe compared to that of the corridor shear walls at the corresponding levels. Typical damage occurred only in the form of screw withdrawal and crushed sheathing corner.

Since the largest story drift demand occurred at level 4 during the pre-fire test sequence (PIDR reached 1.7%), the room-side gypsum panels of the corridor and corner shear walls at the *northwest compartment* of level 4 were removed to allow for inspection of the shear wall framing and steel sheathing. With a measured panel shear distortion of 0.7%, the corridor shear wall underwent localized buckling of the sheathing steel at the top of wall, while the framing studs and tracks did not sustain visible damage (Fig. 10). In addition, loosening of the bolts at the floor bearing connections was detected following the pre-fire earthquake tests. In contrast, the corner shear wall of the same room of level 4 attained a panel shear distortion of < 0.2%. Therefore, no visible damage of either the framing or the sheathing steel was detected (Fig. 11). Comparison of the steel sheathing damage collaborates the differences of the structural panel shear distortion demands between the corridor and corner shear walls.

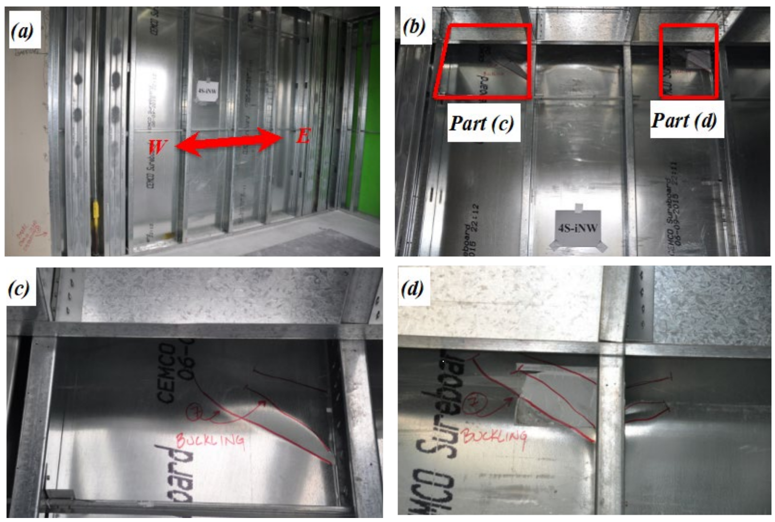

Figure 10. Longitudinal corridor shear wall framing following the pre-fire test sequence: (a) wall framing, (b) localized buckling at the top of sheathing steel, (c) and (d) close-up of the localized buckling.

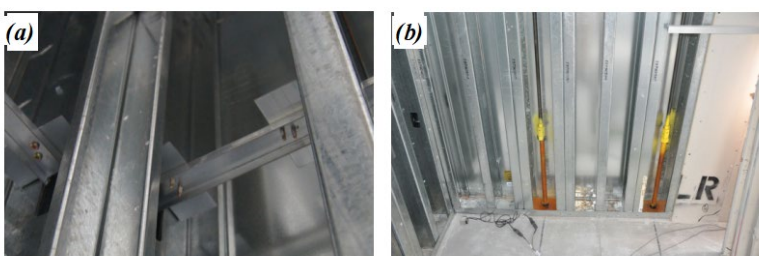

Figure 11. Longitudinal corner shear wall framing following the pre-fire test sequence: (a) upper corner, and (b) bottom track and studs.

6 Conclusions

To advance the state of understanding regarding the seismic performance of mid-rise CFS structures, a full-scale six-story cold-formed steel building was constructed and tested on the UCSD Large High Performance Outdoor Shake Table test facility in 2016. This paper provides a brief overview of the earthquake test program and summarizes the system-level response of the test building. Herein, the paper summarizes the component-level behavior of the shear wall systems including cross-comparison between long-interior corridor walls and shorter exterior walls. Important findings regarding the seismic behavior and physical damage of the shear wall systems in this building-level earthquake test program include the following:

1. The measured panel shear distortions of the corridor shear walls were consistently larger than those of the corner exterior shear walls at the same level. This may be attributed to the fact that very large aspect ratio (> 4:1) of the corridor shear walls may lead to increased flexural deformation and reduced shear deformation during lateral loading. Further experimental studies may be conducted to understand the effect of aspect ratios on the shear wall local behavior.
2. Shear wall segments located at the same wall line and of similar length along the corridor of the building achieved comparable achieved comparable local responses (i.e., structural panel shear distortions, wall end vertical displacements, tie-down rod forces) during the earthquake tests. This indicates that individual corridor shear walls performed as individual wall segments (Type I system) in response to seismic lateral loads. In contrast, the measured local responses of the longitudinal shear walls located at the same wall line appeared less correlated (in particular the tie-down rod axial forces). This may be due to the interaction between the longitudinal corner shear walls with the adjacent transverse shear walls.
3. The shear walls systems at all levels performed satisfactorily during the pre-fire earthquake test phase. However, as a result of different local behavior, in particular smaller panel shear distortion demands, the corner (exterior) shear walls sustained less severe damage compared to the corridor shear walls at the same level. Inspection of the steel sheathing of the shear walls at level 4 revealed the occurrence of buckling of sheathing steel of the corridor shear wall structural panels following the pre-fire earthquake tests, whereas those of the corner shear walls remained undamaged.

Acknowledgements

The test program was a collaboration between two academic institutions (University of California, San Diego and Worcester Polytechnic Institute), two government or institutional granting agencies (Department of Housing and Urban Development and the California Seismic Safety Commission), and 15 industry partners. The Jacobs School of Engineering and Department of Structural Engineering at UCSD also provided matching support for this effort. It is noted that while UCSD led the overall test program with their primary focus was on the earthquake test phases, we are grateful to Prof. Brian Meacham and Dr. Praveen Kamash from WPI for their leading efforts on the fire testing and contribution to the overall test program. In addition, the support of NHERI@UCSD staff as well as individuals who contributed greatly to the specimen construction and testing, in particular Tyler Elliot, Srikar Gunissety, Kelly Holcomb, Diego Riveria, and Fernando Sesma, are greatly acknowledged. Opinions and findings of this study are of the authors and do not necessarily reflect those of the sponsors.

References

AISI (American Iron and Steel Institute) (2007). *North American standard for cold-formed steel farming—Lateral design*. AISI S213, Washington, DC.

AISI (American Iron and Steel Institute) (2012). *North American specification for the design of cold-formed steel structural members.* AISI S100, Washington DC.

Al-Kharat, M., and Rogers, C. (2007). "Inelastic performance of cold-formed steel strap braced walls." *J. Constr. Steel Res.*, 63(4), 460–474.

ASCE (American Society of Civil Engineers) (2010). *Minimum Design Loads for Buildings and Other Structures*. ASCE 7, Reston, VA.

Balh, N., DaBreo, J., Ong-Tone, C., El-Saloussy, K., Yu, C., and Rogers, C. (2014). "Design of steel sheathed cold-formed steel framed shear walls." *Thin-Walled Struct.*, 75, 76–86.

Hutchinson, T.C., Wang, X., Hegemier, G., Meacham, B., Kamath, P., Sesma, F., and Holcomb, K. (2017). "Earthquake and Post-Earthquake Fire Performance of a Mid-Rise Cold-Formed Steel Framed Building." *Proc., 2017 SEAOC Convention*, San Diego, CA.

Liu, P., Peterman, K.D., and Schafer, B.W. (2014). "Impact of construction details on OSB-sheathed cold-formed steel framed shear walls." *J. Constr. Steel Res.*, 101, 114–123.

Serrette, R., Encalada, J., Juadines, M., and Nguyen, H. (1997). "Static racking behavior of plywood, OSB, gypsum, and fiberboard walls with metal framing." *J. Struct. Eng.*, 123(8), 1079–1086.

Shamim, I., Dabreo, J., and Rogers, C. (2013). "Dynamic testing of single- and double-story steel-sheathed cold-formed steel-framed shear walls*." J. Struct. Eng.*, 139(5), 807–817.

Wang, X., Hutchinson, T.C., Hegemeir, G., Gunisetty, S., Kamath, P., and Meacham, B. (2016). Earthquake and post- earthquake fire performance of a mid-rise cold-formed steel framed building - test program and test results: Rapid Release Report. *Report No. SSRP-16/07*. University of California, San Diego. La Jolla, CA.

Wang, X., Hutchinson, T.C., Hegemeir, G., Gunisetty, S., Kamath, P., and Meacham, B. (2018). Earthquake and post-earthquake fire performance of a mid-rise cold-formed steel framed building - test program and test results: Final Report. *Report No. SSRP-16/08*. University of California, San Diego. La Jolla, CA.

Yu, C. (2010). "Shear resistance of cold-formed steel framed shear walls with 0.686 mm, 0.762 mm, and 0.838 mm steel sheet sheathing." *Eng. Struct.*, 32 (6), 1522–1529.